Fluorescence Turn-off Sensor for Selective Determination of Nimesulide Based on Protein Functionalized Gold

Nanoclusters

Zafna Rasheed*a, Shanty Antony Angamaly*b, Anuja Elevathoor Vikramanc, Soumya Thekkedath Cyriacd

*a Department of Chemistry, The Cochin College, Kochi 2, Kerala, India

*b Department of Chemistry and Centre for Research, St Teresa's College, Ernakulam, Kerala, India.

^c Department of Chemistry Govt. Polytechnic College, Perumbavoor.

^d Department of Chemistry and Research Centre, St Albert's College (Autonomous)

Ernakulam.

Abstract

Fluorescence sensing is a highly sensitive detecting method realized through producing an attenuation, enhancement or wavelength shift in the emission. Protein conjugated fluorescent gold nanoclusters (NCs) owe much attention in the field of medical and nanobiotechnology due to their intense and versatile photo stability characteristics. Herein we present a nanosensor with fluorometric readout based on protein-stabilized gold nanoclusters for the selective sensing of the non-steroidal anti-inflammatory drug Nimesulide (NIM). NIM induced a photoluminescence (PL) quenching of BSA-modified gold nanoclusters via an electron transfer mechanism and a novel turn-off sensor was developed. The quenching of fluorescence intensity of BSA stabilised gold nanoclusters allowed the selective determination of NIM in the linear range $1.0 \times 10^{-4} - 5.0 \times 10^{-6}$ M and a limit of detection (LOD) of 6.28×10^{-7} M was obtained. More importantly the developed sensor allowed precise determination of NIM in commercially available pharmaceutical formulations.

Keywords: BSA capped gold nanoclusters, Fluorescence sensor, Nimesulide, Quenching

Introduction

Among nanoprobes, semiconductor-based nanocrystals, including quantum dots, have displayed immense potential as fluorescent imaging probes, however, face limited use due to the toxicity associated with the heavy metals [1]. Among metal-based nanoprobes, gold nanoclusters (AuNCs) have shown wide applications due to their facile synthesis, biocompatibility, limited photobleaching, and bright fluorescence properties [2]. The ultrasmall size, good photostability, and high photoluminescence have gained them a wide range of applications in optical sensing, bio-labeling and catalysis [3-5]. These nanostructures present electronic transitions between HOMO-LUMO energetic levels due to their very small size [6,7]. Because of the quantum confinement effect, they also exhibit size-dependent fluorescence properties [8,9]. These nanoclusters have extremely high extinction coefficients and strongly distance-dependent surface plasmon resonance (SPR) absorption [10,11].

Protein conjugated fluorescent gold nanoclusters have gained much attention in the field of research due to their fascinating chemical and photophysical properties. Luminescence in the visible and near infrared regions is the striking property of these clusters [12,13]. Macromolecular template-based synthesis of clusters is highly recognized due to the non-toxic nature, high bio-compatibility and intense luminescence of the resulting clusters [12,14]. In addition to the above mentioned properties, their easy one-step and environment friendly synthesis makes them particularly attractive [12,15].

Although various proteins have been utilized for cluster synthesis, bovine serum albumin (BSA)-based systems are the most extensively studied [16,17]. Upon the addition of Au (III) ions to the BSA solution, the ions are sequestered and entangled by the BSA molecules, which subsequently reduce them to form stable gold nanoclusters (AuNCs) in situ. These synthesized AuNCs exhibit remarkable stability, and the BSA layer on their surface enables further post-synthetic modifications with functional ligands [18]. Moreover, the intense luminescence of the protein-conjugated clusters allows for highly sensitive quantification of target molecules [19].

Nimesulide (NIM) chemically, 4-nitro-2-phen-oxymethanesulfonamide is a non-steroidal anti-inflammatory drug (NSAID) with antipyretic and analgesic properties and is commonly prescribed for the treatment of acute pain and symptomatic treatment of

osteoarthritis [20]. It inhibits prostaglandin synthetase/cyclo-oxygenase and thereby controls prostaglandin production. It is a free radical scavenger and offer protection against tissue damage that occur during inflammation. It is also effective in relieving the pain associated with rheumatoid arthritis and osteoarthritis [21].

NIM is banned in US, Britain and Canada, but is available in more than 50 countries around the globe [22]. Excess use of NIM causes acute side effects related to gastrointestinal and genitourinary (blood in urine, decrease in urination and kidney failure) systems [20]. It is also associated with side effects such as headache, dizziness, nausea, abdominal discomfort, peripheral edema and hypersensitivity reactions. Therefore, it is essential to develop simple and precise techniques for the determination of NIM in pharmaceutical formulations as drug monitoring has a great impact on public health [22]. The predominant analytical techniques for the assay of NIM includes, chromatography [23], differential pulse voltammetry [24], adsorptive stripping voltammetry [25] and spectrometry [26]. These methods, though sensitive and specific are laborious and so the development of simple, rapid and cost-effective sensors still remains a great challenge. In the present work, we explore the emission properties of BSA capped AuNCs, and its use as a turn-off type fluorescent sensor for the selective determination of NIM, among other NSAIDs such as, mefenamic acid (MEF), diclofenac sodium (DIC), rofecoxib (ROF) and ibuprofen (IBU).

Experimental

Materials and measurements

All the reagents used were of analytical grade. Bovine serum albumin (BSA) was purchased from HiMedia Laboratories Private Ltd., India and chloroauric acid from Spectrochem Private Ltd., India. Pure drugs used in the studies viz nimesulide (NIM), diclofenac sodium, mefenamic acid, ibuprofen and rofecoxib were obtained as gift samples. Pharmaceutical formulations were purchased from local medical store. Milli Q water was used for preparing all solutions. UV-visible spectra were recorded by using Thermoscientific, Evolution 201, China. For fluorescence measurements JAZ-EL-200-X spectrofluorimeter was employed. The FTIR spectra of the samples were recorded on JASCO-4100 FTIR using KBr discs. Morphology of the nanoparticles was investigated by TEM (JEOL/JEM 2100).

Synthesis of BSA stabilized AuNCs

BSA protected AuNCs were synthesized as per the reported procedure [27]. A solution of HAuCl₄.4H₂O (10 mg mL⁻¹) was prepared and 4.1 mL of aqueous HAuCl₄ solution was added to 10 mL BSA solution (50 mg mL⁻¹) under vigorous stirring. Here, vigorous stirring may be attributed for the reduction of Au³⁺ to Au¹⁺, as BSA native protein possess reducing and stabilizing properties. Two minutes later, 1 mL of 1 M NaOH solution was added and the reaction mixture was incubated at 37 °C for 12 hours. A color change in the reaction mixture from dark yellow to reddish brown confirmed the reduction of Au¹⁺ to Au⁰ to form clusters [28]. The resulting deep brown solution exhibited strong red fluorescence under UV light.

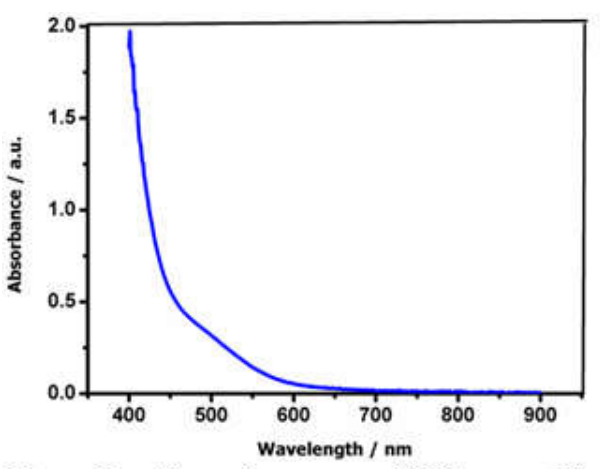
Analytical procedure

The BSA-AuNCs probe was taken in a quartz cuvette and required amount of NIM solution (1.0×10^{-4} to 5.0×10^{-6} M) was added and made up to a total volume of 2 mL by adding 0.1 M phosphate buffer solution (PBS) of pH 8. The fluorescence spectra were recorded at $\lambda_{ex}/\lambda_{em} = 400$ / 640 nm. The luminescence intensity of BSA-AuNCs in the absence and presence of NIM was assigned as I_0 and I respectively and quenching of fluorescence intensity was noted as the ratio I_0 / I.

Results and Discussion

Characterization of synthesized BSA capped AuNCs

The as-synthesised AuNCs which were deep brown color and exhibited bright-red fluorescence did not display a prominent peak in the UV-Vis absorption spectrum, but instead, a weak broad absorption band at around 500 nm was observed and may be due to the quantum size and protein functionalization on its surface [29] (Fig. 1a). The emission at 636 nm can be attributed to the electronic transitions and radiative electron-hole recombination process taking place between the excited 'sp' bands and low lying 'd' bands of AuNCs [30] (Fig. 1b). These nanoclusters exhibited a stokes shift of 150 nm, which could prevent the measurement errors caused by light scattering and self-quenching of fluorescence [31].



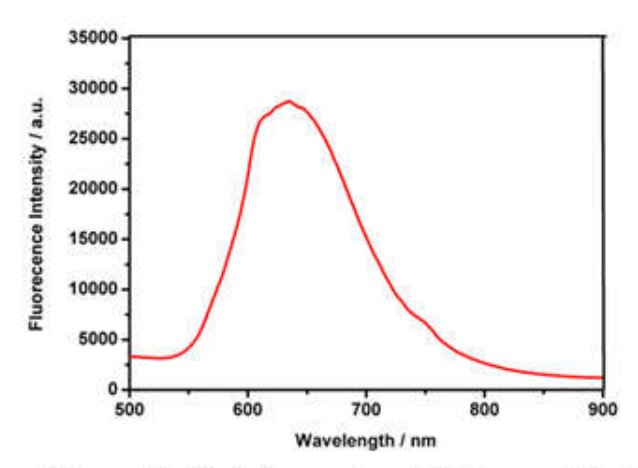


Figure 1a: Absorption spectra of BSA capped AuNCs

Figure 1b: Emission spectra of BSA capped AuNCs

Comparison of the FTIR spectra of BSA and BSA–AuNCs [Fig. 2] shows that the vibrational bands of BSA changed slightly upon the formation of AuNCs. The peaks at 2955 and 3320 cm⁻¹ were due to the C-H and O-H/N-H stretching frequencies respectively. The characteristic amide I band, due to the C=O stretching vibrations and out of phase C-N stretching vibrations was observed at 1640 cm⁻¹. The band observed at 1450 cm⁻¹, (amide II band) may be attributed to the C-N (stretching) vibration with the N-H bending mode. Amide I and amide II bands depicted no significant changes indicating that the AuNCs embedded in BSA did not affect the secondary structure of BSA.

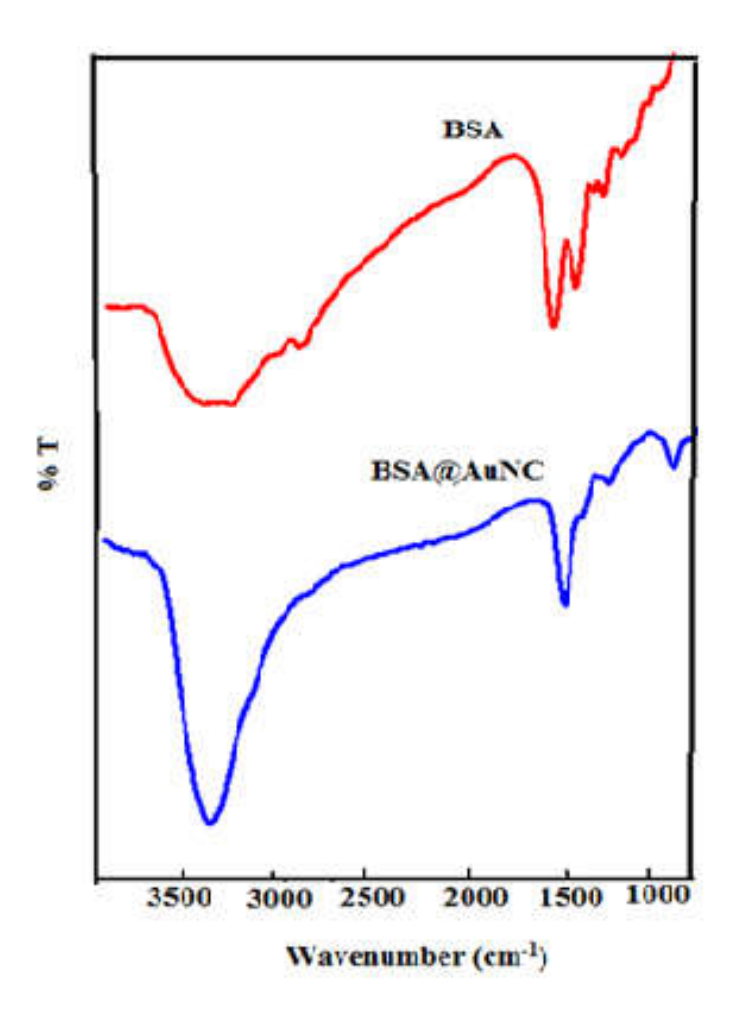


Fig. 2 FTIR spectra of BSA and BSA capped AuNCs

The morphology and particle size of the nanoclusters were assessed by TEM analysis. From the TEM image it is clear that, the particles are spherical, well dispersed and uniform in size with an average diameter of 1.5 nm [Fig. 3].

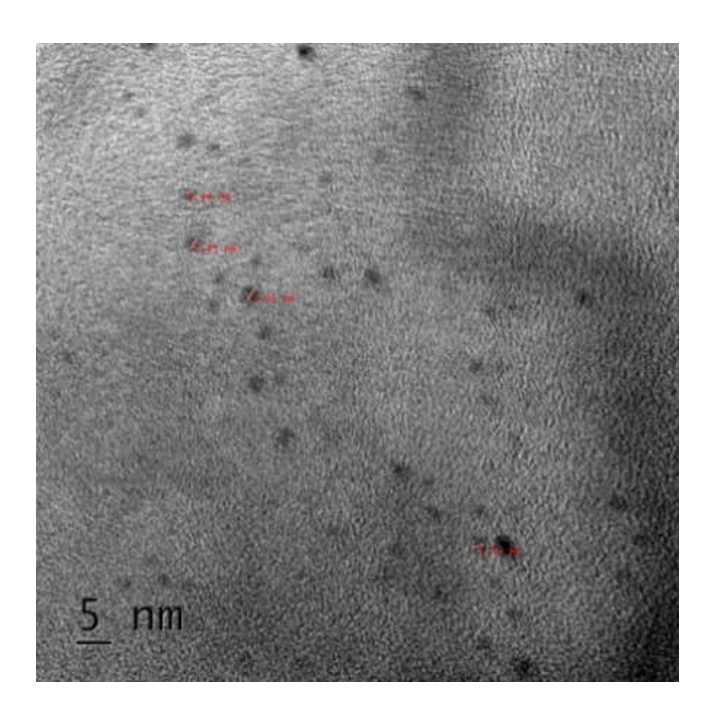


Figure 3: TEM image of BSA capped AuNCs

Fluorescence quantum efficiency of the synthesized nanoclusters was determined using rhodamine 6G as an emission standard. The integrated fluorescence intensity of different concentrations of AuNCs was plotted against absorbance. From the resulting slopes, the quantum yield was calculated using the equation

$$\phi_{AuNCs} = \phi_R \frac{I_{AuNCs}}{I_R} \frac{A_R}{A_{AuNCs}} \frac{\eta_{AuNCs}^2}{\eta_R^2}$$

Where ϕ is the quantum yield, I, the integrated fluorescence intensity, A refers to the absorbance and η is the refractive index of the solvent used. Subscript R represent the reference and AuNCs represents BSA capped gold nanoclusters. The quantum yield of BSA capped AuNCs was found to be 5.3 % which agrees with reported values [32].

Optimization of experimental parameters

Effect of Buffer

The fluorescence quenching of AuNCs by NIM was studied in various buffers (0.1 M citrate buffer, 0.1 M acetate buffer and 0.1 M PBS) and it was seen that maximum fluorescence

quenching and minimum time for stabilisation was obtained with PBS and hence PBS was opted as the medium for further investigations.

Effect of pH

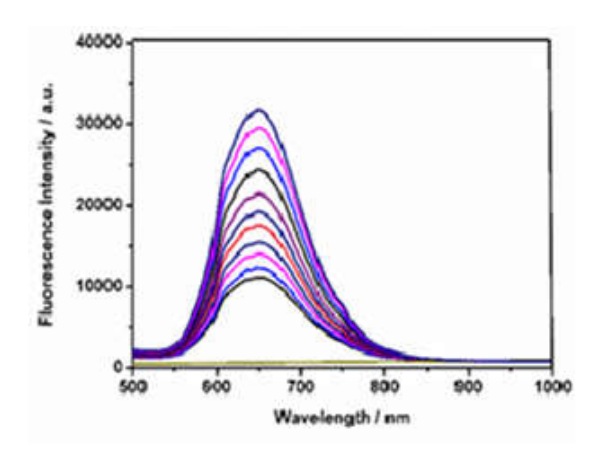
The impact of pH on the emission intensity of AuNCs was investigated both before and after the addition of NIM, as illustrated in Figure 8. At lower pH values (3 to 7), the stability of AuNCs is known to decrease significantly, resulting in reduced quenching efficiency. The greatest fluorescence quenching by NIM was observed at pH 8, making it the optimal pH for the buffer solution.

Effect of dilution

The relative fluorescence intensity (I₀/I) of the AuNCs in the presence of NIM changed with varying dilutions of the probe. Different volume ratios of AuNCs and PBS (pH 8) were used, and I₀/I was measured after adding NIM. The highest I₀/I value was observed when the AuNCs and PBS were mixed in a 1:3 volume ratio.

Performance of the sensor

In order to evaluate the performance of the assay, the fluorescence intensity of AuNCs in the presence of NIM solutions of varying concentrations ranging from $1.0 \times 10^{-4} - 5.0 \times 10^{-6}$ M was measured. A gradual decrease in fluorescence intensity was observed with an increase in concentration of NIM [Fig. 4a]. The limit of detection and limit of quantification were estimated to be 6.28×10^{-7} M and 2.09×10^{-6} M, respectively [Fig. 4b]. The relative standard deviation for six repetitive fluorescence intensity measurements of AuNCs in presence of 1.0×10^{-5} M NIM was calculated to be 1.4 %, suggesting good repeatability for the proposed method.



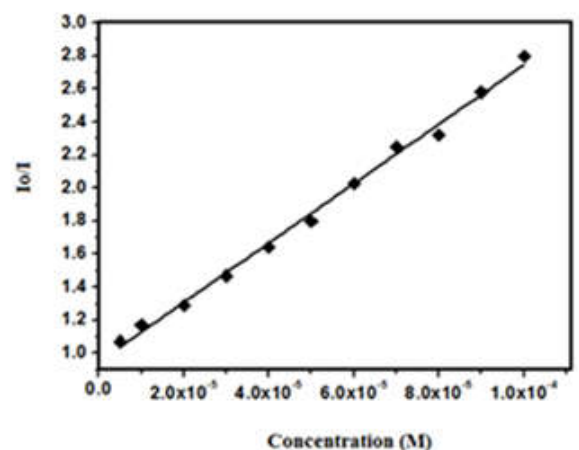


Figure 4a: Fluorescence quenching of AuNCs in the presence of various concentration of NIM (1.0 \times 10⁻⁴ – 5.0 \times 10⁻⁶ M) in 0.1 M PBS (pH 8)

Figure 4b: Calibration plot for NIM in the range $1.0 \times 10^{-4} - 5.0 \times 10^{-6}$ M

Sensing mechanism

A variety of molecular interactions can result in quenching, including excited-state reactions, molecular rearrangements, energy transfer, ground state complex formation, and collisional quenching. It was observed that the absorption spectrum of NIM and emission spectrum of BSA-AuNCs shows no overlapping. Also, the emission spectrum of BSA-AuNCs shows no change in shape upon addition of NIM indicating no possibility for inner filter effect. (33,34,35) Moreover, the absorption band of BSA-AuNCs in presence and absence of NIM showed no observable variation which ascertain that no complex has formed between them. Meanwhile, the maximum emission wavelength was constant with the addition of increasing concentrations of NIM (Figure 5), indicating that the surface state of the BSA-AuNCs has not changed [36].

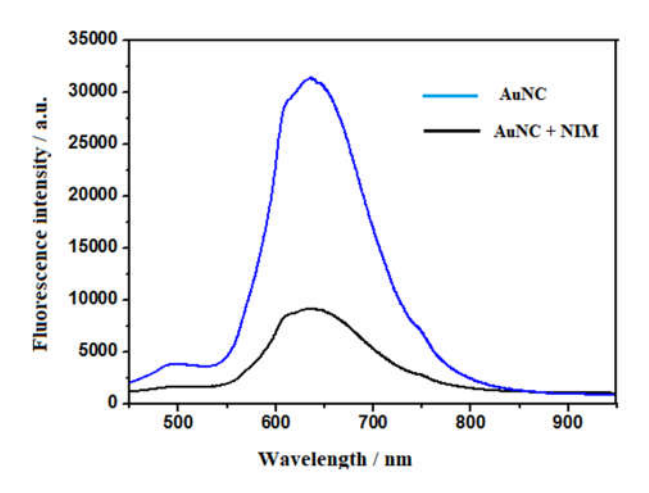


Fig. 5 Fluorescence spectra of AuNCs in the absence and presence of NIM $(1.0 \times 10^4 \text{ M})$

From the time-resolved study a shortening of the average life time of BSA-AuNCs is observed in the presence of NIM. The average lifetime of the nanocluster in the absence and presence of NIM was found to be 15 ns and 11 ns respectively and is in close agreement with the steady-state fluorescence quenching results. This indicates that a nonradiative quenching process is operating due to the electronic interaction of AuNCs with NIM. The non-radiative relaxation method mainly proceeds via either electron transfer or energy transfer pathways. Since there is no overlapping between absorption spectrum of NIM and emission spectra of BSA-AuNCs, quenching is not due to the fluorescence resonance energy transfer (FRET). Therefore, the nonradiative relaxation of the AuNCs upon addition of NIM is due to the electron transfer mechanism. It has been already established that electron transfer is more favorable to electron-deficient species and can occur from the excited fluorophore to the quencher [37]. The presence of nitro group on NIM further confirms the mechanism of quenching as electron transfer process [Fig. 6].

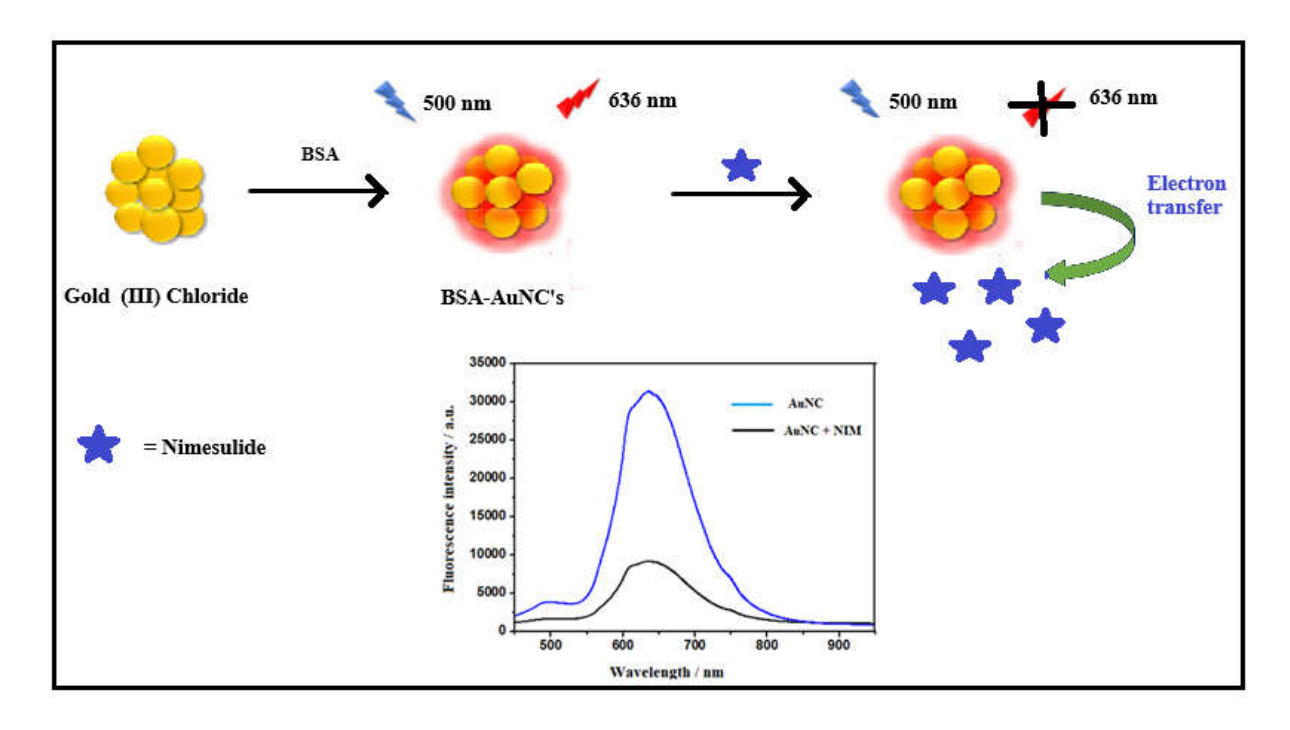


Fig. 6 Schematic representation of the sensing of NIM using BSA-AuNC's

Selectivity

One of the most significant properties of a sensor is its selectivity. To study the selectivity of the probe, different species $(5.0 \times 10^{-5} \text{ M})$ that are either structurally related, similar in function or coexisting were taken and their effect on the fluorescence intensity of probe was studied. NSAIDs such as mefenamic acid (MEF), rofecoxib (ROF), ibuprofen (IBU), diclofenac sodium (DIC) and possible coexisting substances such as ascorbic acid, citric acid, urea, glucose, lactose, Na⁺, K⁺, SO₄²⁻ and Cl⁻ were used for the selectivity study. Among these only NIM was found to effectively quench the fluorescence intensity of the probe whereas all others caused weak fluorescence variations. The change in fluorescence response of AuNCs upon the addition of above mentioned NSAIDs is shown in Figure 6. These results suggest that the proposed sensor possessed high selectivity towards NIM and has the potential for practical detection of NIM in real samples.

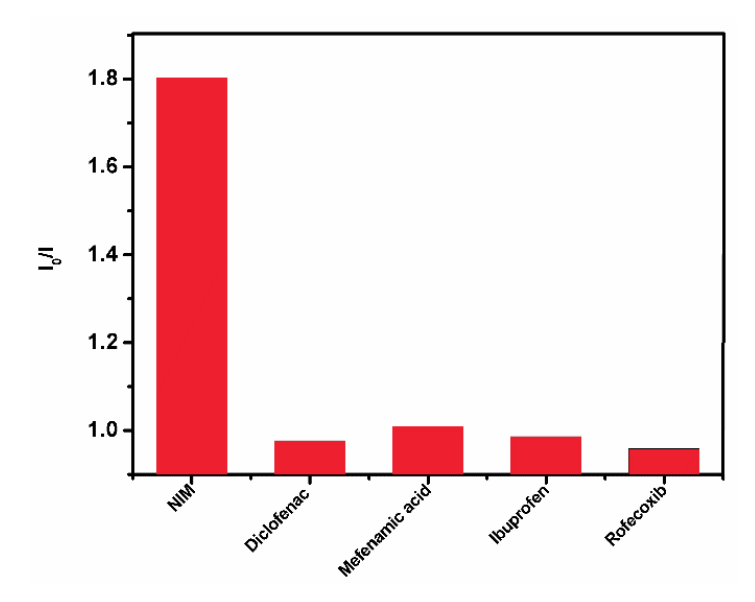


Fig. 6 Selectivity of the sensor

Furthermore, the effect of concentration of above-mentioned species in the fluorescence sensing of NIM was studied. Except ascorbic acid (which exhibited an enhancement upon addition to BSA-AuNCs) none of the species studied showed significant interference (signal change above 5%) even when present up to 100 fold excess.

Application Studies

The practical utility of the proposed sensor, was tested by using the method for the determination of NIM in commercially available pharmaceuticals. The experimental results are compared with the standard method for NIM analysis [38] and are presented in Table 1. The good agreement between found and declared values of NIM in pharmaceutical sample indicates accuracy of the developed sensor. The good recovery and lower RSD value obtained from the application studies conducted using the proposed sensor thereby confirms its practical utility in real sample analysis. These findings confirmed that the developed method afforded good precision, accuracy and recovery which reveals its effectiveness.

Sample	Declared amount (mg/Tablet)	Method adopted	Found* (mg/Tablet <u>+</u> R.S.D.)
Nimcip (Cipla)	100.0	Proposed method	100 ± 0.2
		Standard method	100 ± 0.4
		(Potentiometric titration)	

^{*}Average of six replicates

Table 1: Determination of NIM in pharmaceutical sample

Conclusion

A highly sensitive and selective fluorometric sensor was developed for the drug NIM based on fluorescence quenching of BSA capped AuNCs induced by NIM. The assay allowed sub micro-molar determination of NIM with good reproducibility and repeatability. A linear correlation between fluorescence quenching ratio and concentration of NIM was obtained in the range $1.0 \times 10^{-4} - 5.0 \times 10^{-6}$ M and the detection limit was estimated to be 6.28×10^{-7} M. The assay exhibited excellent selectivity towards NIM among other NSAID's and was successfully applied to the determination of NIM in pharmaceutical formulations.

Reference

- 1. V. Jain, S. Bhagat, S. Singh, Sens. Actuators B Chem., 327, 128886 (2021)
- Z. F. Pu, J. Peng, Q. L. Wen, Y. Li, J. Ling, P. Liu, Q. E. Cao, *Dyes Pigm.*, 193, 109533 (2021)
- 3. H. W. Li, Y. Yue, T. Y. Liu, D. Li, Y. Wu, J. Phys. Chem. C., 117, 16159 (2013)
- 4. L. Yang, P. Hou, J. Wei, B. Li, A. Gao, Z. Yuan, Molecules, 29, 1574 (2024)
- 5. N. El-Sayed, M. Schneider, J. Mater. Chem. B., 8, 8952 (2020)
- 6. M. Zhu, C.M. Aikens, F.J. Hollander, G.C. Schatz, *J. Am. Chem. Soc.* 130 (18) 5883–5885 (2008)
- 7. S. Zhu, X. Wang, Y. Cong, L. Li, ACS Omega, 5, 22702 (2020)

- 8. S. Han, Z. C. Zhang, S. P. Li, L. M. Qi, G. M. Xu, Sci. China-Chem., 59, 794-801 (2016)
- 9. A. Cantelli, G. Battistelli, G. Guidetti, J. Manzi, M. Di Giosia, M. Montalti, *Dyes Pigment.*, 135, 64-79 (2016)
- 10. X. He, H. Liu, Y. Li, S. Wang, Y. Li, N. Wang, J. Xiao, X. Xu and D. Zhu, *Adv. Mater.*, 17, 2811 (2005)
- 11. L. Chen, M. Gharib, Y. Zeng, S. Roy, <u>C. K. Nandi</u>, <u>I. Chakraborty, Mater. Today</u>
 Chem., 29, 101460 (2023)
- 12. M. S. Mathew, A. Baksi, T. Pradeep, K. Joseph, *Biosens. Bioelectron.*, 81, 68 (2016)
- 13. G. Zhang, B. Fang, <u>J. Peng</u>, S. Deng, L. Hu, <u>W. Lai, Chem. Eng. J.,</u> 503, 158294 (2025)
- 14. J. J. Feng, H. Huang, D. L. Zhou, L. Y. Cai, Q. Q. Tu, A. J. Wang, *J. Mater. Chem. C*, **1**, 4720 (2013)
- C. A. J. Lin, T. Y. Yang, C. H. Lee, S. H. Huang, R. A. Sperling, M. Zanella, J. K. Li, J. L. Shen, H. H. Wang, H. I Yeh, W. J. Parak, W. H. Chang, *ACS Nano*, 2, 395 (2009)
- 16. A. Baksi, P. L. Xavier, K. Chaudhari, N. Goswami, S. K. Pal, T. Pradeep, *Nanoscale*, 5, 2009 (2013)
- 17. T. Das, P. Ghosh, M. S. Shanavas, A. Maity, S. Mondal, P. Purkayastha, *Nanoscale*, **19**, 6018 (2012)
- 18. C. Banerjee, J. Kuchlyan, D. Banik, N. Kundu, A. Roy, S. Ghosh, N. Sarkar, *Phys. Chem. Chem. Phys.*, **16**, 17272 (2014)
- 19. Y. Wang, J. Chen, J. Irudayaraj, ACS Nano, 5, 9718 (2011)
- 20. M. Govindasamy, V. Mani, S. Chen, T. Maiyalagan, S. Selvaraj, T. Chen, S. Lee, W. Chang, *RSC Adv.*, 7, 33043 (2017)
- 21. A. Bernareggi, *Inflammopharmacology*, **9**, 81, (2001)
- 22. S. Menon, K. Girish Kumar, J. Electrochem. Soc., 164, B482 (2017)
- 23. R. Makhmudov, F. Yunusov, *Pharma Innovation*, 10, 1 (2021)
- C. Wang, X. Shao, Q. Liu, Q. Qu, G. Yang, X. Hu, J. Pharmaceut. Biomed. Anal.,
 42, 237 (2006)
- 25. M. Łysoń, A. Górska, B. Paczosa-Bator, R. Piech, Electrocatalysis, 12, 641 (2021)

- 26. D. Thomas, L. Lonappan, L. Rajith, S. T. Cyriac, K. Girish Kumar, *J. Fluoresc.*, **57**, 267, (2009)
- 27. Z. Chen, S. Qian, X. Chen, W. Gao, Y. Lin, *Analyst*, **137**, 4356 (2012)
- 28. Y. Negishi, K. Nobusada, T. Tsukuda, J. Am. Chem. Soc., 127, 5261 (2005)
- S. Govindaraju, S. R. Ankireddy, B. Viswanath, J. Kim, K. Yun, Sci. rep., 7, 40298
 (2017)
- 30. J. Zheng, J. T. Petty, R. M. Dickson, J. Am. Chem. Soc., 125, 7780 (2003)
- 31. H. H. Lin, Y. C. Chan, J. W. Chen, C. C. Chang, J. Mater. Chem., 21, 3170 (2011).
- 32. C. T. Yuan, W. C. Chou, J. Tang, C. A. Lin, W. H. Chang, J. L. Shen, D. S. Chuu, *Opt. Express*, **17**, 16111 (2009)
- 33. U. Sivasankaran, S. T. Cyriac, S. Menon, K. Girish Kumar, *J. Fluoresc.*, **27**, 69 (2017).
- 34. A. R. Jose, U. Sivasankaran, S. Menon, K. Girish Kumar, *Anal. Methods.*, **8**, 5701 (2016)
- 35. M. Maity, S. Dolui, N. C. Maiti, Phys. Chem. Chem. Phys., 17, 31216 (2015)
- 36. Z. Chen, S. Qian, J. Chen, J. Caia, S. Wua, Z. Cai, Talanta, 94, 240 (2012)
- 37. J. R. Lakowicz, *Principles of Fluorescence Spectroscopy*, 3rd edn, Springer, USA (2006)
- 38. European Pharmacopoeia 4th ed. France 1531 (2002)